GeoScienceWorld
Lithosphere
Volume 2022, Article ID 10.2113/2022/6306735, 12 pages
https://doi.org/10.2113/2023/10.2113/2022/6306735

Lithosphere

Research Article

Characteristics and Geological Implications of Lacustrine Carbonate of Nantun Formation in Hailar Basin

Tong Lin,[1,2] **Zonglun Sha**,[2] **Kedan Zhu**,[3] **Jinhao Nan**,[2] **Yanguang Ren**,[2] **and Baoshuai Li**[4]

[1]*Chengdu University of Technology, Chengdu, Sichuan 610059, China*
[2]*Exploration and Development Research Institute, Daqing Oilfield Company Limited, Daqing, Heilongjiang 163712, China*
[3]*PetroChina Hangzhou Research Institute of Geology, Hangzhou, Zhejiang 310023, China*
[4]*Daqing Oilfield Company Limited, Daqing, Heilongjiang 163712, China*

Correspondence should be addressed to Tong Lin; ltong0118@163.com

Received 31 May 2022; Revised 12 January 2023; Accepted 21 January 2023; Published 21 April 2023

Academic Editor: Shuangpo Ren

Globally, lacustrine carbonate rocks are often found in rift lake basins. Because they often do not form large-scale conventional or unconventional reservoirs, they have not received enough attention in previous oil and gas exploration. Recent years, exploration examples in China show that lacustrine carbonate has close relationship with unconventional oil and gas. Mudstone with carbonate deposits always has a good exploration effect in the area. However, the genesis of lacustrine carbonate is still controversial. The sediment environment difference between carbonate and mudstone and its effects on unconventional hydrocarbon accumulation are not yet clear. This paper focuses on lacustrine carbonate found in the Nantun Formation in Hailar Basin. Through the analysis of lithofacies, geochemistry, and logging data, several findings have been obtained in the current study. (a) Two kinds of lacustrine carbonates, micrite dolomite and marlstone, which represent semideep to deep lake environments, have been identified in the research area. (b) Lacustrine dolomite (LD), whose genesis may relate to magmatic movement and deep hydrothermal processes, shows an extremely dry, hot paleoclimate and a saline, anaerobic ancient water condition. (c) Carbonate deposition in mudstone is related to the condensation section, and marlstone and micrite dolomite represent the beginning and end of the condensation section, respectively. Compared with mudstone around carbonate rocks, LD represents a drier, hotter, and saltier environment, which is of significance for sedimentary environment identification. In addition, the mudstone with lacustrine carbonate deposits has better organic matter characteristics and can form good unconventional oil and gas reservoirs that are of great significance for further exploration.

1. Introduction

Recently, the continued rise of the oil price and the urgent demand for hydrocarbon resources have promoted the study of unconventional oil and gas reservoirs. Generally, lacustrine carbonates are not typical unconventional reservoir types. However, carbonate minerals, such as dolomite, have good reservoir properties and brittleness. What's more, in a salty environment, which is favorable for carbonate deposition, shale always has high-quality hydrocarbon-generating ability. All these factors make lacustrine carbonate that is sandwiched in shale or mudstone to be a new focus in the study of unconventional reservoir research.

Dolomite and limestone can be found not only in marine environments but also in nonmarine lacustrine sediments worldwide. The genesis of lacustrine carbonate, especially LD, is the most controversial problem. The main explanations are about primary dolomite [1], penecontemporaneous dolomite [2], microbial dolomite [3–5], hydrothermal dolomite [6, 7], and so on. Micrite dolomite deposits in saline lake; Coorong Lagoon in western Victoria, Australia, is considered to be a typical primary dolomite [1, 8]. Micrite dolomite associated with gypsum in Sanmenxia Sag, Dongying Sag, Qinyang Sag, and Qikou Sag in China is considered related to the evaporation of the penecontemporaneous period [9]. Dolomite deposits

in black organic-rich sediments at ambient temperatures on the surface of the Lagoa Vermelha Lagoon near Rio de Janeiro, Brazil, were referred to as the microbial dolomite model [10]. Lacustrine exhalative rocks associated with hydrothermal minerals were discovered in the Cretaceous of the Jiuxi Basin and the Permian of the Santanghu Basin in China [11–13]. They were considered to be primary dolomite related to deep hydrothermal fluids and fracture systems. All these genesis models of LD correspond to different lithologies, lithology combinations, and associated mineral combinations. Thus, to correctly evaluate and understand the genesis and indicative significance of lacustrine carbonate rocks in a study area, restoring the diagenesis environment of lacustrine carbonate is very important.

Lithofacies analysis is the most direct way to determine the sedimentary environment, but when it comes to paleoclimate judgment, this method has great limitations. The accumulation of carbonate deposits in an ocean or lake basin is controlled by physical and chemical parameters such as temperature, pH, pressure, and carbon dioxide content in the water [14, 15]. These differences will be directly reflected in the trace element distribution and ratio of the sediments. Especially in the lacustrine sedimentary system, the effect is more significant. Therefore, it is a reliable means to reflect paleoclimate and paleowater condition changes of lake basin by analyzing the difference of trace elements in lacustrine carbonate rocks. But this kind of analysis is more focused on each point where sampled. For a more continuous and macroscopic understanding of differences in sedimentary environments between lacustrine carbonate and shale, we need to combine sequence stratigraphy.

Milankovitch cycles are the smallest high-frequency sequence units that correspond to climatically derived sedimentary cycles at rhythmic levels [16, 17]. Logging curve is the most direct and accessible material for time series analysis, which has the characteristics of effective sampling, continuous data, and high resolution. However, due to the influence of many different levels of cyclic external forces and complex geological processes, it is often difficult to visually decompose and identify different levels of stratigraphic sequences by using conventional logging curves directly. In 2005, the integrated prediction error filter analysis (INPEFA), a spectral attribute trend analysis technique for stratigraphic analysis, appeared abroad. The corresponding commercial software, CycloLog, was launched, which was very practical in the rapid identification of different levels of sequence interfaces [18, 19].

In the past, lacustrine carbonate rocks and shale were always studied separately [20–23]. However, recent exploration in China has shown that shale oil production is more related to shale lithofacies, mineral types (such as dolomite), inorganic interlayers, maturity, formation pressure, and fracture development. The traditional view on the relationship between oil production and shale thickness and organic matter content is controversial [24, 25]. Since 2018, China has made breakthroughs in shale oil exploration in the Permian strata of Jimsar Sag in Junggar Basin [26–28] and Kondian Formation in Bohai Bay Basin [29]. These fine-grained sedimentary rocks are developed in saline lake basins and contain more dolomite content, which further clarifies that the development of lacustrine carbonate rocks is closely related to shale oil and gas.

Hailar Basin is an Early Cretaceous continental extensional fault-depression lake basin system, but there were never any reports on lacustrine carbonate in an exploration or development history of more than 60 years [30]. And the study of shale oil and gas is just in its infancy. This paper started with cores and thin sections and combined with geochemical and logging data, analyzed the sedimentary environment of lacustrine carbonate rocks in Hailar Basin comprehensively, and discussed its sequence stratigraphic connotation in lake basin evolution and its geological significance for unconventional oil and gas.

2. Geological Setting

Hailar Basin is located in the Hulunbuir League, Inner Mongolia autonomous region in China (Figure 1(a)). It is an extensional-compressional type Mesozoic-Cenozoic continental sedimentary basin that is superimposed on the Paleozoic collision orogen of the Inner Mongolia-Greater Khingan Mountains. Hailar Basin can be divided into five first-order tectonic units with two uplifts and three depressions and twenty secondary order units with four uplifts and sixteen sags (Figure 1(b)). During the Lower Cretaceous, four stages of basin-forming periods (Figure 1(c)): rifting period, fault-depression transition period, depression period, and inversion depression period [31]. Tamulangou Formation was formed during the initial rifting period, as represented by a large number of volcanic eruptions of Xing'anling Group. Tongbomiao Formation was formed during the expansional rifting period, a set of gray-green and gray conglomerates intercalated with tuffaceous siltstone, fine sandstone, and mudstone strata developed. Nantun Formation was formed during the strongly rifting period. In the early and middle stages of this period (N1 member of Nantun Formation), thick gray, dark gray, and even black mudstone intercalated with siltstone and argillaceous siltstone. And in the late stage (N2 member of Nantun Formation), gray and dark gray mudstones developed. Damoguaihe Formation was formed during the fault-depression transition period, and interbedded gray mudstone, argillaceous siltstone, and siltstone were developed. Yimin Formation was formed during the depression period, dominated by fluvial delta facies that developed siltstone, sandstone, and conglomerate.

3. Materials and Methods

3.1. Material. There are two main sources of samples in this paper: 30 samples were collected from wells of Hailar Basin and 47 data results were obtained through literature research about other basins (Table 1). Samples' lithology in Hailar Basin includes calcareous mudstone, marl, micrite dolomite, and mudstone. They were collected from Well C2 and X15 mainly in N1 member of Nantun formation. In

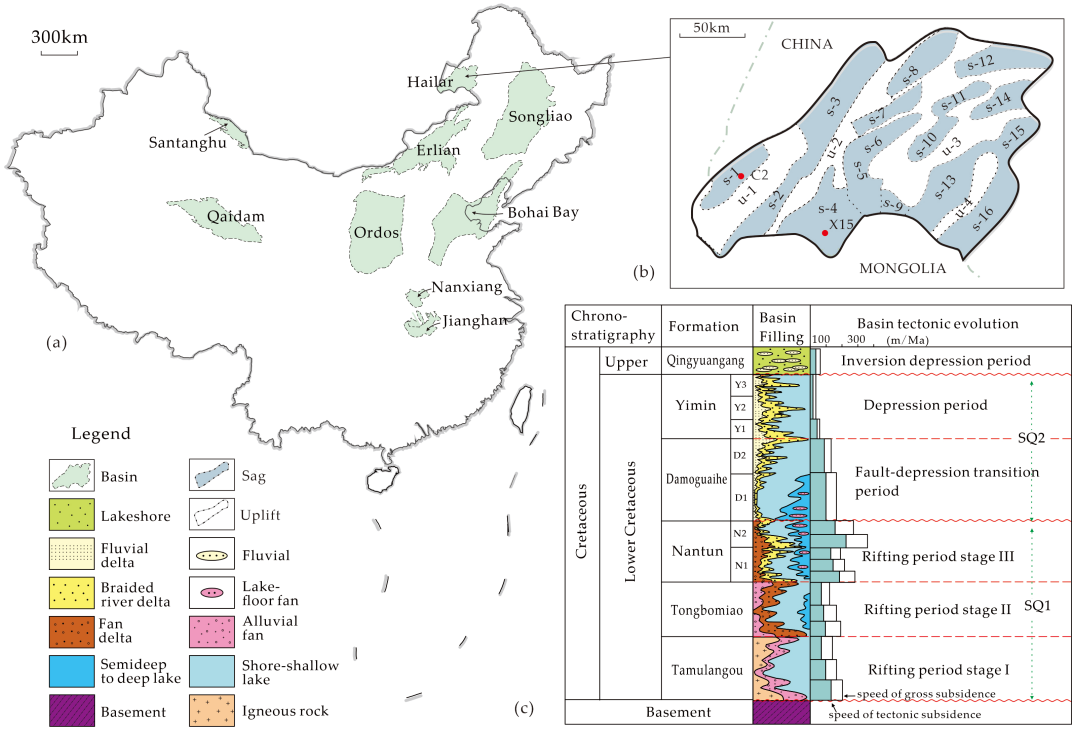

FIGURE 1: (a) Basins that have LD developed in China. (b) Tectonic setting of Hailar Basin (s-1, Bayanhushu Sag; s-2, Chagannor Sag; s-3, Hulunhu Sag; s-4, Beier Sag; s-5, Wuerxun Sag; s-6, Xinbaoli Sag; s-7, Hongqi Sag; s-8, Herhongde Sag; s-9, Wuyi Sag; s-10, Modamuji Sag; s-11, Wugunor Sag; s-12, Dongming Sag; s-13, Huhehu Sag; s-14, Ewenke Sag; s-15, Yimin Sag; s-16, Jiuqiao Sag; u-1, Hanhula uplift; u-2, Cuogang uplift; u-3, Bayanshan uplift; u-4, Xilinbeir uplift) and location of wells used in paper (C2, X15). (c) Stratigraphy of Lower Cretaceous Formation in Hailar Basin.

addition, research data from other papers are mainly about dolomite; they came from Erlian Basin, Ordos Basin, Bohai Bay Basin, Jianghan Basin, and Liaohe Basin [32–36].

3.2. Analytical Methods. All experiments and analyses were done at Exploration and Development Research Institute in Daqing Oil Field. Samples from Hailar Basin were identified by core observation and thin-section analysis; eighteen of them were tested for principal and trace elements. An S4 PIONEER X-ray fluorescence spectrometer was used during principal and trace element testing at a room temperature of 25°C and humidity of 30%.

INPEFA processing of logging curves can accurately compare high-frequency sequences by analyzing the trend patterns and inflection point types of different levels of curves. Sequence boundaries (SBs) and flood surfaces of different levels can be determined by this method, and then changes in the sedimentary environment can be recognized [19, 37]. The first step of INPEFA is spectrum analysis of logging curves. Maximum entropy spectrum analysis (MESA) is used here to extrapolate the autocorrelation function according to the maximum information entropy criterion. The second step is prediction error filtering analysis (PEFA). On the basis of MESA, the PEFA curve can explain the continuity of the formation. It can be obtained by calculating the difference between the MESA-predicted value and the actual value of the corresponding logging curve of each depth point. The third step is to obtain the INPEFA curve by applying a specific integration process to the PEFA curve. A positive trend indicates that the predicted value in the moving window is lower than the actual value of the curve. A negative trend indicates that the predicted value in the moving window is higher than the curve value.

This paper uses CycloLog software for INPEFA processing. Considering the content of mudstone can directly reflect the depth of lake water. By selecting logging curves sensitive to the change of mudstone content, the trend of the INPEFA curve obtained can better show the change of lake water level. In general, the natural gamma ray logging curve can better reflect the change of argillaceous content. However, affected by volcanism during the rifting period, a large section of gray tuffaceous siltstone and gray-green tuffaceous mudstone can be found in the southern section of Hailar Basin [38]. Tuffaceous had high radioactivity, which caused natural gamma ray (GR) logging value to be too high, misleading the estimation of argillaceous content. Therefore, this paper selected GR curve for Well X15, which does not contain tuff matter, to build INPEFA curve. But for Well C2, which has a large change in tuff matter content from bottom to top, potassium element curve in GR spectrum logging was selected to analyze the trend of INPEFA. A positive trend represents that the actual mudstone content is higher than predicted in this period, which is a transgression stage or a flood stage. On the contrary, a negative trend represents the period

Table 1: Information on samples used in this study.

Basin	Well	Quantity	Lithology	Source
Hailar	C2, X15	30	Micritic dolomite/dolomitic mudstone/mudstone/sandstone/limestone	This study
Erlian	A23, et al.	12	Dolomitic mudstone/dolomite	[12, 32]
Ordos	TS-03	1	Dolomite	[33]
Liaohe	L59, et al.	6	Micritic dolomite/dolomitic mudstone/calcareous dolomite/argillaceous dolomite	[36]
Jianghan	W1	18	Argillaceous dolomite/dolomitic mudstone	[34]
Bohai Bay	T12c	10	Dolomite	[35]

when the actual mudstone content is lower than predicted, that is, when the actual sandstone content is more. This indicates a process of regression [19, 39].

4. Results

4.1. Petrography. The lacustrine carbonate rocks discovered in Hailar Basin are all developed at the top of N1 member of Nantun Formation with thin thickness. Two lithologies have been identified by core observations, thin-section identification, and principal element analysis (Table 2); one is gray micrite dolomite with lamellar mud, the other is gray black marlstone. Considering that lacustrine carbonate rocks are relatively thin and distributed in mudstone in the form of interlayers, this paper divided samples into four types to compare the changes of depositional environment. They are LD, adjacent mudstone (AM) whose distance less than 30 cm with LD, same oilgroup mudstone (SM) whose distance less than 10 m with LD, different oilgroup mudstone (DM) whose distance more than 200 m with LD

4.2. Micrite Dolomite. The dolomite in this section is interbedded between dark gray mudstone and gray siltstone with a thin thickness of about 0.2 m (Figure 2(a)). Thin-section identification results show that it has a dark-bright interlamellar (Figure 2(b)). The bright layer is mainly micrite dolomite with some powder crystal dolomite, about 0.01 mm in size (Figure 2(c)). The dark layer is dominated by argillaceous micrite dolomite with phosphate nodules, and framboidal pyrite can be seen bedding (Figure 2(d) and 2(e)). The morphology of these laminas is characterized by disturbance (Figure 2(f)). And these disturbances are gradually reduced to a horizontal shape from bottom to top in this section (Figure 2(b)). There are no terrigenous detritus and gypsum in dolomite, and there are few bioclastic structures.

4.3. Marlstone. Marlstone is sandwiched between gray-black mudstone and silty mudstone with a thickness of about 0.1–0.5 m in each single layer (Figure 2(g)), and brittle fractures are generally developed. When using 5% hydrochloric acid for identification, core samples can form dense bubbles. Microscopic identification showed that the marlstone is mixed with silty quartz from a terrestrial source. The content of quartz is about 1%–10% and gradually decreases as depth shallow in thin sections. These quartzes are angular or subangular and poorly rounded (Figure 2(h)). Framboidal pyrite can also be seen in marl, with a size of 0.1–0.3 cm and a content of 3%–15%. In addition, marl had organic matter layers that differed from dolomite sections (Figure 2(i)).

4.4. Trace Element. The results of trace element are presented in Table 3. It showed different ranges in these four lithology types, and many trace elements, such as Sr, Cu, Ba, Cr, V, Ni, and Rb, had obvious extreme values near the dolomite.

In Nantun formation, the general range of Sr content is 277.5–696.8 ppm, and the Sr content is as high as 880 ppm in dolomite. The general range of Ba content is 323.2–562.1 ppm, while in dolomite, the Ba content is as low as 235 ppm. The general range of Cr content is 28–46.5 ppm, while in dolomite, the Cr content is as low as 16.3 ppm. V content is generally in the range of 47.6–126.4 ppm, but the content is as low as 36.4 in dolomite. Ni content is generally in the range of 11.9–28.2 ppm, and in dolomite, the content is as low as 10.7 ppm. The general range of the Rb content is 105.5–202.6 ppm, while in dolomite, the Rb content is as low as 29.3 ppm.

The ratio of trace elements also showed a sensitive value in dolomite section. For most of the samples, Sr/Cu range is 11.04–43.03 and Sr/Ba range is 0.7–1.48. However, it reached a high value of 53.66 and 3.74 in dolomite. And for Rb/K, V/Cr, and V/(V + Ni), it showed a different pattern. In LD, AM, and DM, the value range of Rb/K, V/Cr, and V/(V + Ni) is about 0.0042–0.0061, 2.23–2.79, and 0.76–0.85, respecitively. But after the sediment of dolomite, it has fallen into a low range in SM that is about 0.0036–0.0042, 1.35–1.79, and 0.68–0.8 (two samples closer to the dolomite were excluded).

4.5. The Integrated Prediction Error Filter Analysis. The INPEFA curve based on natural gamma logging and potassium curve of GR spectrum logging can reflect the variation of mud content so as to judge the change of lake level and SB. It can be seen from Figure 3 that the INPEFA curves of Well X15 and Well C2 show a similar change pattern. Both of these wells can identify two third-order SBs (SB1 and SB4), three fourth-order cycles (SB1-SB2, SB2-SB3, and SB3-SB4), and multiple fifth-order cycles in Nantun Formation. Lake water kept rising during the deposition between N1I and N1III zone and remained at a

Table 2: Results of principal component analysis.

Type	Depth (m)	Fe_2O_3 (%)	Mn (%)	Ti (%)	CaO (%)	K_2O (%)	S (%)	P (%)	SiO_2 (%)	Al_2O_3 (%)	MgO (%)	Na_2O (%)	Lost (%)
LD	1150.4	8.28	0.56	0.15	26.95	0.85	0.03	0.04	25.76	4.47	13.37	1.01	18.36
AM	1150.7	3.47	0.04	0.50	2.39	3.35	0.08	0.33	56.86	14.44	2.87	2.06	13.40
	1150.3	3.52	0.02	0.56	0.78	3.69	0.05	0.09	62.84	15.67	2.32	1.94	8.33

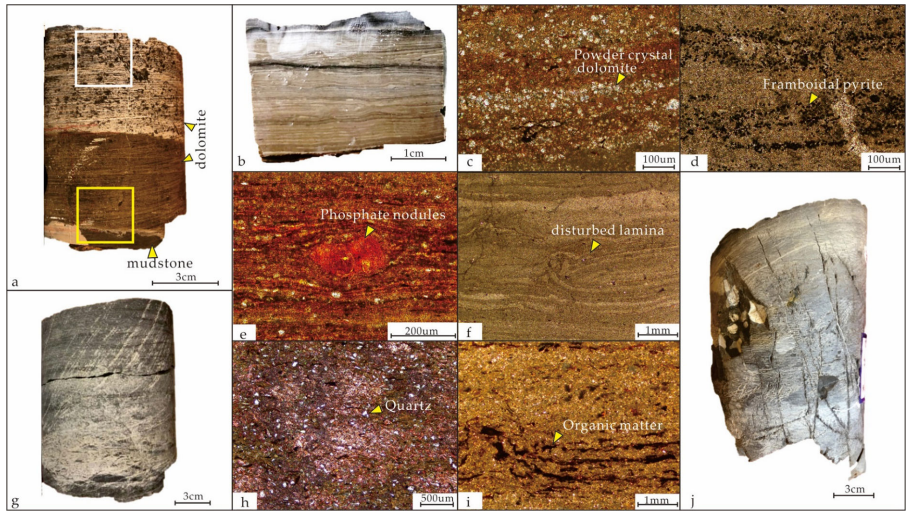

Figure 2: Characteristic of lacustrine carbonate in first member of Nantun Formation, Hailar Basin (well locations were marked in Figure 1). (a) Contact relationship between micrite dolomite and mudstone (yellow rectangle marked), Well C2, 1150.4 m. (b) Core cutting shows laminar features of micrite dolomite, Well C2, 1150 m (sample comes from part of core in (j)). (c) Powder crystal dolomite distributed along the layer (rock slice of (b)), Well C2, 1150 m. (d) Framboidal pyrite distributed laminar (sample comes from part of core in (a) marked with yellow rectangular), Well C2, 1150.6 m. (e) Phosphate nodules, Well C2, 1150.7 m. (f) Disturbing lamina (sample comes from part of core in (a) marked with white rectangular), Well C2, 1150.4 m. (g) Feature of marlstone, Well X15, 2893.98 m. (h) Quartz distributed in marlstone, Well X15, 2893.98 m. (i) Organic matter layers, Well X15, 2891.83 m. (j) Cracks in micrite dolomite, Well C2, 1150 m.

relatively high position during the deposition of N10 zone. After the deposition of N10 strata, lake water gradually receded. The maximum flooding surface (MFS) appears at the middle of N10 strata. Comparing the lacustrine carbonate rocks with the location of MFS, it is found that dolomite develops above MFS in Well C2, and limestone develops below MFS in Well X15.

5. Discussion

5.1. Sedimentary Environment. The instability of lake water or the process of sorting and weathering will cause differences in trace elements in sediments. Trace element testing is a basic method for sedimentary environment analysis and dolomite genesis research. The ratio of trace elements can be used to study the changes in paleoclimate conditions, paleowater conditions, and redox environment during the formation of dolomite in the study area.

5.1.1. Paleoclimate Conditions. Through the comparison of indicators such as Fe/Mn, Mg/Ca, Sr/Cu, and so on, Lijun Song determined that Sr/Cu value was a reliable climate discriminating index [33]. Since the content of Sr was sensitive to paleoclimates, its high value is generally related to the concentration of lake water under dry and hot climates. Therefore, Sr/Cu value is often used to reflect paleoclimate environment. Usually, the ratio indicated a warm and humid climate when it is between 1.3 and 5. And reflected a dry and hot climate while it is greater than 5.0 [40–42].

In Figure 4(a), we can found that paleoclimate when dolomite or dolomitic mudstone deposit was hot and dry and even reached the peak in this period. The Sr/Cu value of Lower Cretaceous dolomite in Erlian Basin is between 2.24 and 59.14, with an average of 19. It means the dolomite mainly deposits in a dry and hot environment, with partially formed a humid climate. Lijun Song concluded that Sr/Cu value of dolomite is 13.94 in Ordos Basin and reflected a relatively dry and hot climate environment. The study area in this paper is a small rifted lake basin; either Sr or Cu contents in water body are more sensitive to the climate change. The average value of Sr/Cu of AM, which deposits above or below LD is 12.67. However, Sr/Cu value of dolomite reached 53.66 and reflected short-term dry-hot or even

Table 3: Trace element test analysis results.

Type	Depth (m)	Sr (ppm)	Cu (ppm)	Ba (ppm)	Cr (ppm)	V (ppm)	Ni (ppm)	Rb (ppm)	Sr/Cu	Sr/Ba	Rb/K	V/Cr	V/(V + Ni)
LD	1150.4	880.0	16.4	235.0	16.3	36.4	10.7	29.3	53.66	3.74	0.0042	2.23	0.77
AM	1150.3	340.0	30.8	426.0	46.5	126.4	24.9	179.8	11.04	0.80	0.0059	2.72	0.84
	1150.7	472.0	33.0	441.0	44.4	120.8	26.8	164.5	14.30	1.07	0.0059	2.72	0.82
SM	1142.6	460.9	13.3	555.2	28.0	50.1	23.1	115.6	34.76	0.83	0.0041	1.79	0.68
	1143.4	553.9	15.0	502.3	28.8	47.6	11.9	115.8	36.83	1.10	0.0040	1.65	0.80
	1144.4	455.2	12.3	515.7	36.1	48.6	13.6	112.3	36.92	0.88	0.0040	1.35	0.78
	1145.8	517.8	12.3	522.5	38.3	56.1	19.3	116.1	42.00	0.99	0.0040	1.46	0.74
	1146.8	407.5	9.5	562.1	34.6	51.3	17.5	114.1	43.03	0.72	0.0038	1.48	0.75
	1147.8	404.1	14.6	539.7	38.5	57.6	16.0	118.1	27.71	0.75	0.0039	1.50	0.78
	1148.8	357.1	13.9	509.1	37.8	51.3	21.0	105.5	25.78	0.70	0.0036	1.36	0.71
	1149.6	351.8	23.8	399.3	43.5	94.7	17.8	157.3	14.79	0.88	0.0052	2.17	0.84
	1150.1	318.8	18.9	329.3	41.9	99.3	27.1	131.5	16.84	0.97	0.0051	2.37	0.79
DM	1397.0	277.5	17.7	323.2	35.7	80.8	14.3	170.9	15.70	0.86	0.0061	2.26	0.85
	1398.0	594.8	19.7	503.5	36.5	82.1	22.8	171.9	30.27	1.18	0.0058	2.25	0.78
	1398.7	355.9	17.3	462.6	36.8	95.7	28.2	202.6	20.61	0.77	0.0056	2.60	0.77
	1399.7	696.8	19.8	531.9	30.4	78.8	21.3	156.6	35.21	1.31	0.0054	2.59	0.79
	1400.7	682.3	23.9	461.0	30.1	84.0	22.9	137.7	28.60	1.48	0.0055	2.79	0.79
	1401.8	492.1	21.2	380.0	28.7	78.1	24.5	152.1	23.25	1.30	0.0055	2.72	0.76

extremely dry-hot climate conditions in lake basin during the depositional period of dolomite in N1 member of Nantun Formation.

5.1.2. Paleosalinity Conditions. Since the contents of K, Rb, Sr, Ba, and other elements are significantly different in marine and continental sediments, the contents or ratios of these elements are often used to distinguish sedimentary environments, especially changes in paleosalinity [43]. The commonly used indicators are Sr/Ba and Rb/K. When the ratio of Sr/Ba is greater than 1, it reflected saltwater environment, and when the ratio is lower than 0.6, it reflected freshwater environment. And for the ratio of Rb/K, it represented marine sedimentary environments when the value is greater than 0.006 and indicated freshwater environment if value is less than 0.004 [40].

In Table A1, we can find that previous studies had showed Sr/Ba values of Jianghan Basin, Bohai Bay Basin, Liaohe Basin, and other places are generally higher than 1, which characterized a saltwater environment. The test results of samples in Erlian Basin vary greatly, ranging from 0.20 to 2.97, with an average ratio of 1.15, which is characterized by both fresh and saltwater (Figure 4(b)).

By comparing the Sr/Ba value of LD, AM, SM, and DM in Well C2 in Hailar Basin, all of mudstone sample values are relatively concentrated, ranging from 0.70 to 1.48, with an average ratio of 0.97, reflecting transitional environment between brackish water and salt water. Due to characteristics of high Sr and low Ba, dolomite section showed a more prominent high Sr/Ba value (up to 3.7). Considering that strontium can displace calcium easily and accumulate in calcite or aragonite, it can also lead to a high Sr/Ba value in lacustrine carbonate, so we judge paleosalinity by the reference to Rb/K value [44–47]. In Hailar Basin, the minimum ratio of Rb/K was 0.0036, the maximum ratio was 0.0061, and the average ratio was 0.0049. These values manifest as numerical scattered between different oil groups, relatively concentrated in same oil group (Figure 4(c)). The Rb/K value of dolomite sample is 0.0042, which is similar to Rb/K value of SM samples. But it showed a relatively high value in samples that are adjacent to dolomite (AM) that reflected a brackish environment in that period and a process of increasing salinity of lake water before or after dolomite deposition.

5.1.3. Redox Environment. V/Cr values and V/(V + Ni) values are more commonly used for judging redox conditions. The high-valent ions of V and Cr can be reduced and enriched in the environment of hypoxic denitric acid, while Ni is mainly enriched in sulfate reduction environment. It is generally believed that the ratio of V/Cr reflected the hypoxic (reduced) environment when the value is greater than 4.25 and reflected oxidative environment when the value is less than 2. The V/(V + Ni) ratio can not only reflect redox conditions of the sedimentary water body but also the water stratification. Generally, ratio greater than 0.84 represents a strongly stratified hypoxic environment, between 0.54 and 0.82 represents a moderately stratified anaerobic environment, between 0.46 and 0.60 represents a weakly stratified oxygen basin-forming poor environment, and less than 0.46 represents an oxygen-rich environment [48–50].

In order to eliminate the judgment error of a single element, two discriminant indicators were comprehensively analyzed. The V/Cr value of dolomite section is 2.23, the V/(V + Ni) value is 0.77, which is an anaerobic

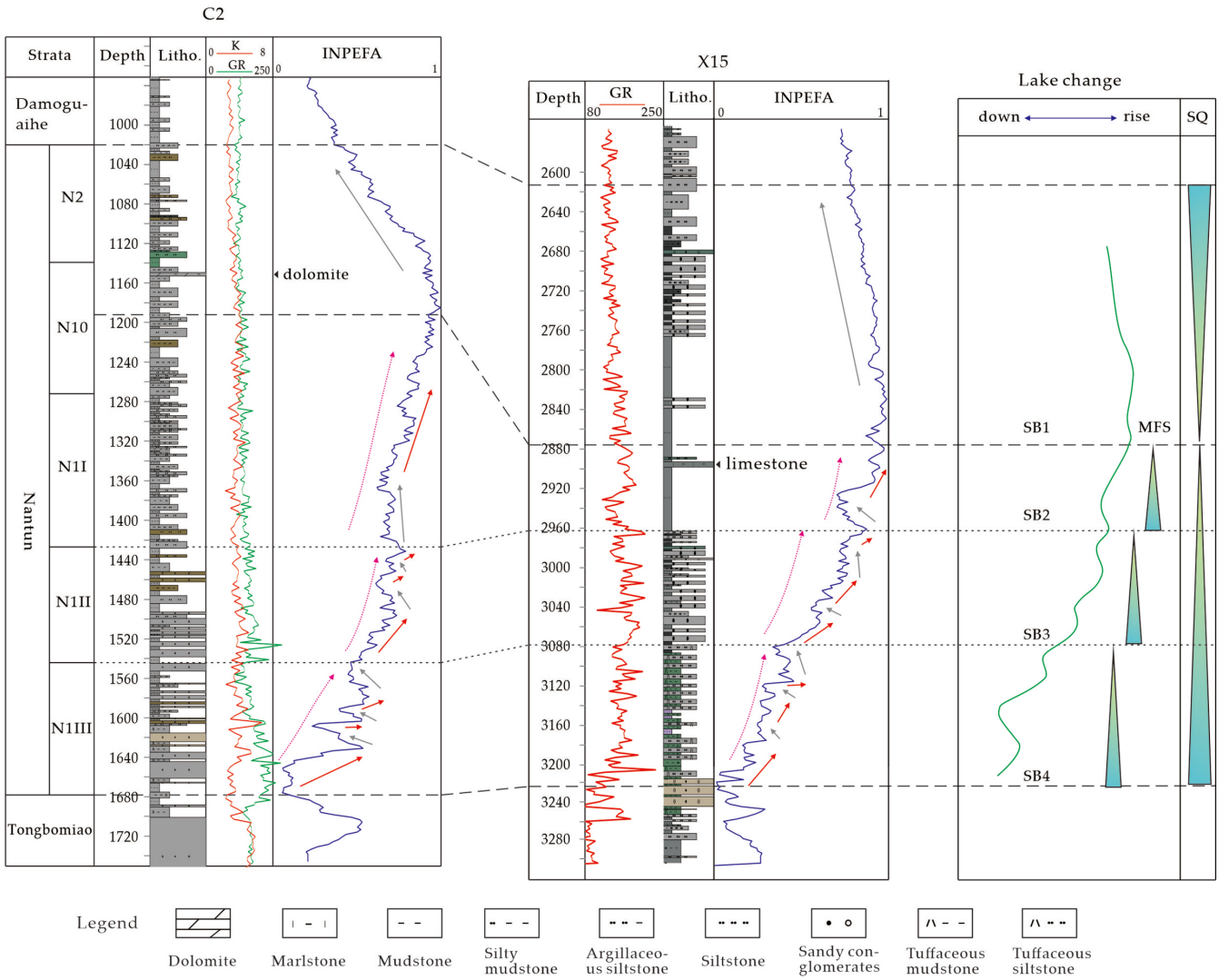

Figure 3: Comprehensive column of lake level change depended on INPEFA in Hailar Basin.

environment. The V/Cr value of the mudstone in same layer (SM) is about 1.35–2.72, and the value of V/(V + Ni) is about 0.68–0.84, which is generally characterized by a weak oxidation to anaerobic environment of moderate stratification. While the mudstone adjacent to dolomite (AM) is a strongly stratified anaerobic to reducing environment, reflecting the increase in oxygen content of lake water during the deposition of dolomite (Figure 4(d)). There may be a process of transient descent of water bodies.

5.2. Geological Significance

5.2.1. Sequence Stratigraphy. Condensed section is a stable sedimentary unit with very thin thickness and low sedimentation rate. It is the symbol of sequence division and the key of sequence stratigraphic correlations. In the Nantun period, Hailar Basin suffered a strong fracture structural action. According to the INPEFA curve, lake level raised in N1 period and reached MFS in N0 period. With a rapid subsidence of the basin and increase of capacity space, the insufficient supply of material sources led to undercompensated starvation deposits in subsidence center of basin. Thus formed a stable and wide distributed condensed section, with a well logging characteristic of "three highs and one low" (high natural gamma ray, high resistivity, high acoustic, and low density), which can be compared and identified in this region [51].

When calibrating the deposited position of lacustrine carbonate rocks, it can be found that their development in the study area corresponds to the MFS. Limestone developed below the MFS, and dolomite developed above the MFS.

According to statistics, the marlstones in Well X15 were all developed in thick layers of gray-black mudstones at N0 member. Terrestrial quartz can be seen in multiple marlstone thin sections. And quartz has a decreasing trend over time, which reflected the process of lake level rising and provenance influence weakening. Combined with INPEFA curve, limestone developed below MFS, reflecting the beginning of the condensed section.

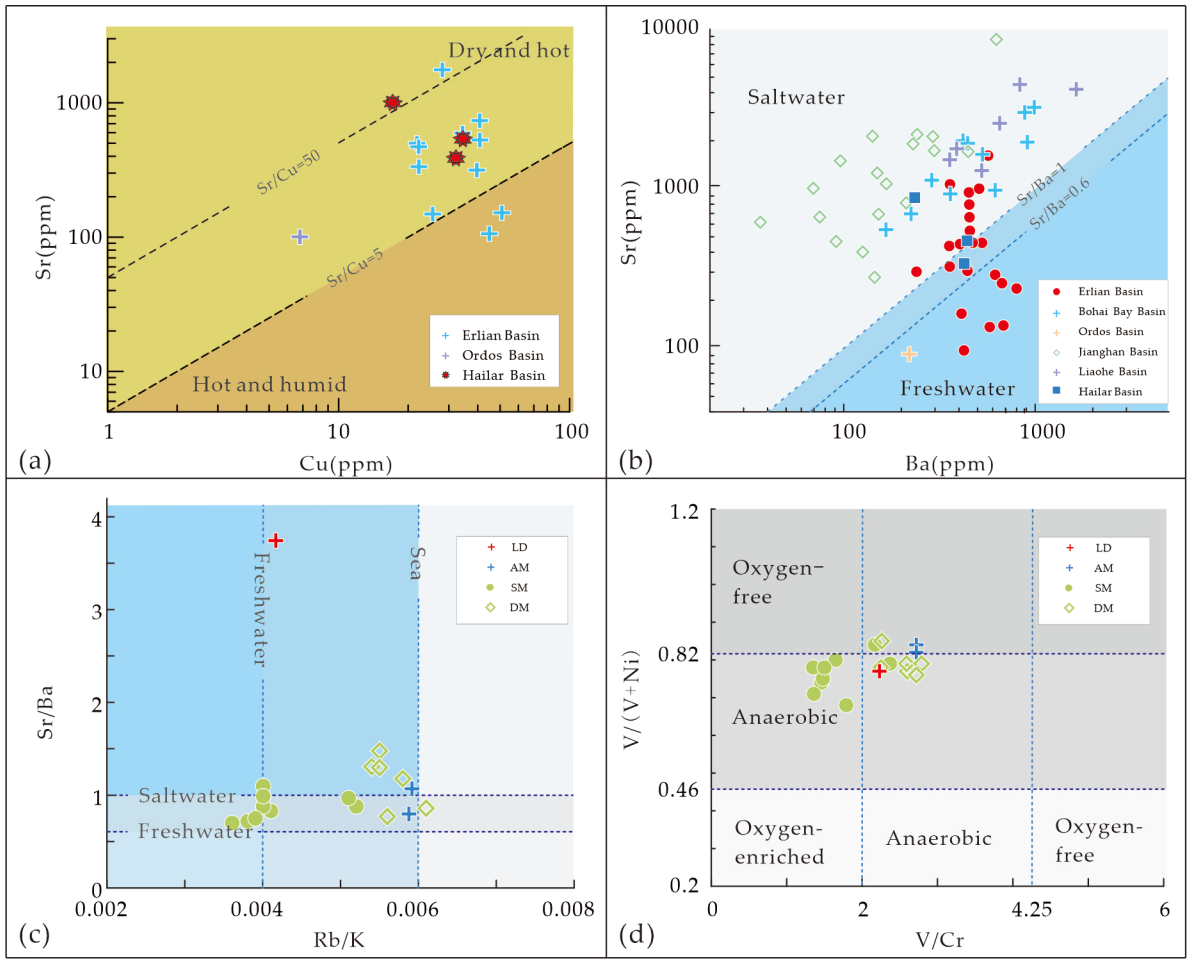

FIGURE 4: Sedimentary environment characteristics indicated by trace elements, data from Table 3 and Table A1. (a) Paleoclimate condition distribution map in different basins. (b) Paleowater condition distribution map in different basins. (c) Differences of Paleowater condition between four types of rocks in Hailar Basin. (d) Redox environment difference between four types of rocks in Hailar Basin.

The micritic dolomite in Well C2 has different characteristics from marlstone in Well X15. In the vertical position, dolomite developed above MFS. Its geochemical indicators were abrupt compared with the upper and lower mudstones (Figure 5). In lithofacies, the laminae of dolomite section mostly had disturbance characteristics, which proved that the sediment environment was not as stable as the high stand system. Lake water began to decline during this period, and micritic dolomite might be a sign of the end of condensed section in Hailar Basin.

5.2.2. Genesis of Lacustrine Dolomite. At present, there are two kinds of understanding about the genesis of LD in the world: primary and secondary. Modern primary dolomite is mainly related to salt lake, evaporation, or micro-organism. Secondary genesis is related to penecontemporaneous metasomatism, magma, hydrothermal fluid, and so on. Hailar Basin, Erlian Basin, Songliao Basin, and Bohai Bay Basin belong to the same Early Cretaceous continental extensional fault basin system with a similar tectonic background. But there are different opinions about the genesis of dolomite.

The LD of Tengger Formation in Erlian Basin is dominated by micritic texture, with laminated and syngenetic deformation structures. It is a jet-type hot-water dolomite related to magmatic activity [32, 52, 53]. The Nenjiang Formation in Songliao Basin is dominated by patchy dolomite, which consists of crystals with cloudy center and clear rims. It is a penecontemporaneous metasomatic genesis [54]. The mineral composition of Bohai Bay Basin is mainly dolomite, analcime, clay minerals, and terrigenous quartz. It is considered that the intrusion of seawater increases the salinity of lake water and promotes the formation of LD [35].

The LD in Hailar Basin mainly developed in semideep lake with simple texture, which is dominated by mud crystal structure, thin in layer, without organic matter and gypsum salt. Therefore, it is mainly dolomitization caused by secondary genesis. Geochemistry shows that the dolomite section is characterized by high Sr/Ba and high Sr/Cu, which are characterized by salt water and extremely dry and hot environment. The generation of this extreme environment may be related to transgression, magma, and so on. Considering that the transgression

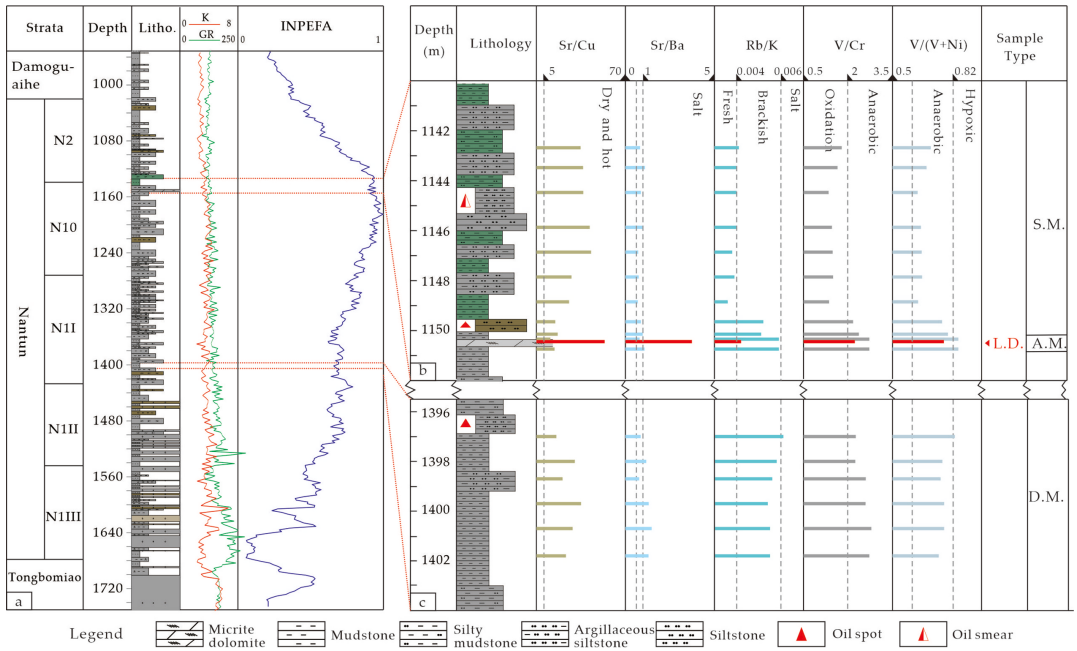

FIGURE 5: Vertical distribution of trace element in Well C2. (a) Strata column and location of (bb) and (c); (b) part of LD, AM, and SM; (c) part of DM.

will cause the discovery of terrigenous materials such as quartz in rock composition as in Bohai Bay Basin. But no relevant components were observed in the micritic dolomite in the study area, thus excluding the influence of transgression. In addition, affected by the large-scale acidic volcanic eruption in the Greater Khingan Mountains, tuff, tuffaceous mudstone, or tuffaceous siltstone was widely developed in basin during the Nantun period [55]. Well C2 is located on the west side of the basin, closer to the Greater Khingan Range and more vulnerable to the impact of volcanism. It is believed that the LD in Hailar Basin has a similar genesis with Tengger Formation in Erlian Basin that is related to magmatism and deep hydrothermal action.

5.3. Hydrocarbon Significance. It can be concluded from previous study that the development of lacustrine carbonate rocks is related to the condensed section. The condensed section is a concept of sequence stratigraphy and is the product of slow deposition stage of basin. It had the electrical characteristics of "three highs and one low" (high natural gamma ray, high resistivity, high acoustic, and low density). During that period, deposition rate is extremely slow, so the deposits are relatively thin. Fangju Chen once evaluated and compared the source rocks of marlstone and ordinary mudstone in Bell Sag of Hailar Basin and found that the marlstone in Nantun Formation had better hydrocarbon generation index such as organic kerogen type, total organic carbon, and hydrocarbon potential. The hydrogen exponent, degradation potential, hydrocarbon expulsion factor, and aggregation factor were more than 1.5 times higher than those of ordinary mudstone layers [51]. It can be seen that the condensed section with lacustrine carbonate rocks had better hydrocarbon generation potential than ordinary mudstones and are favorable source rocks.

Bell Sag is a mature oilfield with rich drilling data. Through the statistics of wells, it is found that the reservoirs are distributed in Beizhong, Beixi, and Sudert areas. When the reservoir profile and marl thickness map are superimposed, it can be found that the reservoir distribution in Bell Oil Field has a good matching relationship with marl thickness (Figure 6). The oil-source correlation results in Table A2 show that crude oil in Bell Sag in Hailar Basin belongs to mature oil and has a good relationship with the samples of marlstone (ω (TOC) > 2.0%) in Nantun Formation. The expulsion efficiency of source rocks in marlstone is high, which is four to six times that of ordinary mudstone. The chloroform bitumen "A" method was used to recalculate the resources of Beixi Subsag, and the result was 213.68 million tons, which is 110.0 million tons more than the resources before the discovery of marlstone [51].

The lacustrine carbonate rocks are mostly intercalated in black shale. Even though pores are not easily developed in lacustrine carbonate rocks, this type of rock is relatively easy to form microcracks (Figure 2(j)). These microcracks are not only a favorable storage space but also important oil and gas migration channels. It provides a new idea that lacustrine carbonate is important for the seeking of high-quality tight oil and gas reservoir.

7. Conclusions

This study set out to illustrate the sedimentary characteristics of lacustrine carbonate rocks. Through petrography, trace element analysis, and logging data, the following

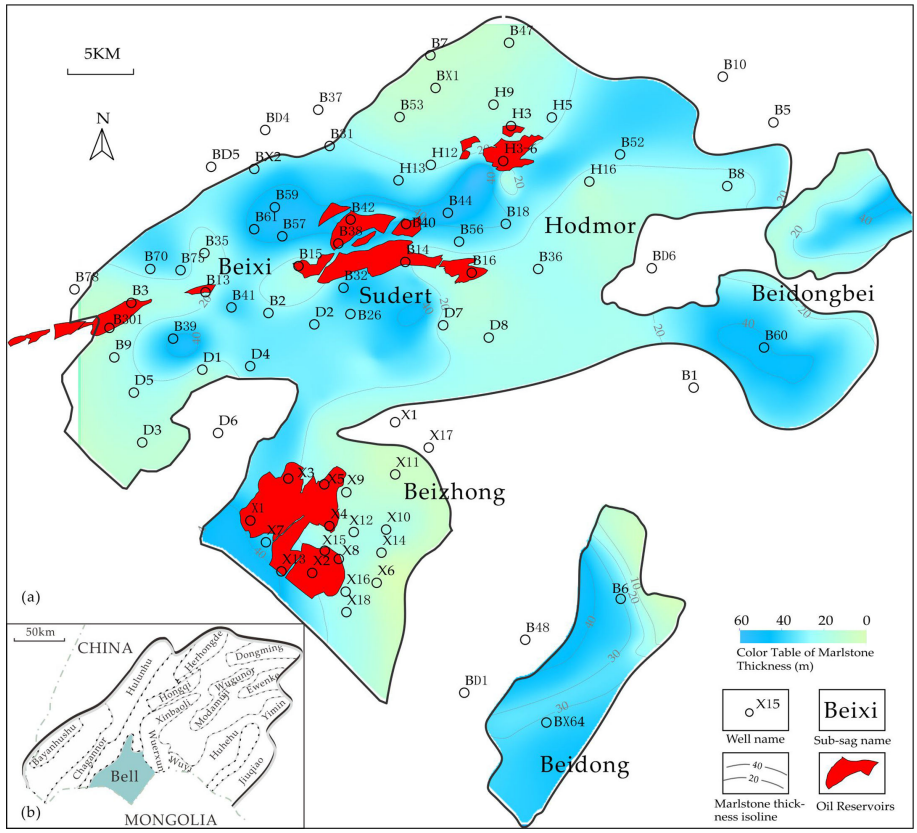

Figure 6: (a) Composite map of marlstone strata and oil reservoirs in Bell Sag (data from the wells marked on the figure). (b) Location of (a) in Hailar Basin.

conclusions are drawn for lacustrine carbonate in Hailar Basin of Nantun Formation:

(1) Two kinds of lacustrine carbonate, micrite dolomite, and marlstone, have been identified in research area. It represents semideep to deep lake environment.

(2) LD shows extremely dry and hot paleoclimate and saline and anaerobic ancient water conditions. Its genesis is related to magmatic movement and deep hydrothermal process.

(3) Carbonate deposition in mudstone is related to condensation section; marlstone indicates the beginning of condensation section and micrite dolomite indicates the end of condensation section.

This study was limited by the lack of dolomite data found in Hailar Basin and cannot carry out more in-depth research with unconventional oil and gas reservoirs. Notwithstanding these limitations, the study suggests that the condensation section with lacustrine carbonate rocks has better oil and gas generation potential than ordinary mudstone. Moreover, lacustrine carbonate rocks have good brittleness and are easy to produce cracks, which are conducive to the accumulation and migration of oil and gas. Therefore, in the case of more sufficient data in the future, more detailed research can be carried out on the carbonate rocks developed in the mudstone of the lake basin, and there will be great gains.

Data Availability

All data used in this research are listed, it can easily accessible by downloading the various documents cited in the paper.

Conflicts of Interest

The authors declare no conflict of interest.

Acknowledgments

The authors greatly appreciate the Exploration and Development Research Institute of Daqing Oilfield Company for providing samples and data access and for permission to publish the results, and appreciate Chen Fangju for providing the relevant information in Figure 6.

Supplementary Materials

Table A1 is a specific list of data mentioned in Table 1 in the "Material" section. It is about the results of trace element analysis of lacustrine carbonate in various basins. These data are collected from the literature. The source of

the literature is marked in Table 1, and the location of the basin is marked in Figure 1. These data are used to compare the results from the study area to discuss the sedimentary environment in "Discussion" section.

Table A2 is the main basic data of Figure 6, which is derived from F. Chen [51]. It lists statistical intervals for each parameter, including minimum value, maximum value, mean value, and number of samples. Used to compare the hydrocarbon index between marlstone and ordinary mudstone.

References

[1] D. T. Wright, "The role of sulphate-reducing bacteria and cyanobacteria in dolomite formation in distal ephemeral lakes of the Coorong region, South Australia," *Sedimentary Geology*, vol. 126, nos. 1–4, pp. 147–157, 1999.

[2] Z. Huang, H. Bao, J. Ren, et al., "Characteristics and genesis of dolomite in Majiagou Formation of Ordovician, south of Ordos Basin," *Geoscience*, vol. 25, no. 5, pp. 925–930, 2011.

[3] J. Fu, B. Wang, L. Sun, et al., "Dolomitization of Ordovician Majiagou Formation in Sulige region, Ordos Basin," *Petroleum Geology & Experiment*, vol. 33, no. 3, pp. 266–273, 2011.

[4] A. Mastandrea, E. Perri, F. Russo, A. Spadafora, and M. Tucker, "Microbial primary dolomite from a norian carbonate platform: Northern Calabria, southern Italy," *Sedimentology*, vol. 53, no. 3, pp. 465–480, 2006.

[5] V. P. Wright, "Lacustrine carbonates in rift settings: The interaction of volcanic and microbial processes on carbonate deposition," *Geological Society, London, Special Publications*, vol. 370, no. 1, pp. 39–47, 2012.

[6] D. Lavoie, "Hydrothermal dolomitization in the Lower Ordovician Romaine Formation of the Anticosti Basin: Significance for hydrocarbon exploration," *Bulletin of Canadian Petroleum Geology*, vol. 53, no. 4, pp. 454–471, 2005.

[7] D. Zhu, Z. Jin, and W. Hu, "Hydrothermal recrystallization of the Lower Ordovician dolomite and its significance to reservoir in northern Tarim Basin," *Science China Earth Sciences*, vol. 53, no. 3, pp. 368–381, 2010.

[8] C. C. Borch and J. B. Jones, "Spherular modern dolomite from the Coorong area, South Australia," *Sedimentology*, vol. 23, no. 4, pp. 587–591, 1976.

[9] C. Huang, J. Yuan, L. Wu, et al., "Origin and research methods of lacustrine dolomite," *Lithologic Reservoirs*, vol. 28, no. 2, pp. 7–15, 2016.

[10] J. Warren, "Dolomite: Occurrence, evolution and economically important associations," *Earth-Science Reviews*, vol. 52, nos. 1–3, pp. 1–81, 2000.

[11] Y. Liu, J. Xin, M. Yuan, et al., "Primary dolostone formation-related to mantle-originated exhalative hydrothermal activities, Permian Yuejingou section, Santanghu area, Xinjiang, NW China," *Science China Press: Earth Science*, vol. 41, no. 12, pp. 1862–1871, 2011.

[12] H. Wen, *Geochemical Characteristics and Genesis of Lacustrine "White Smoke Type" Hydrothermal Sedimentary Rock in Qingxi Sag, Jiuquan Basin*, Docter, Chengdu University of Technology, 2008.

[13] H. Li, Y. Liu, H. Liang, et al., "Origin of lacustrine dolostones of the middle Permian Lucaogou Formation in Santanghu basin of Xinjiang," *Journal of Palaeogeography*, vol. 14, no. 1, 2012.

[14] R. Revelle and R. Fairbridge, "Chapter 10: carbonates and carbon dioxide," in *Treatise on Marine Ecology and Paleoecology*, J. W. Hedgpeth, Ed., 67V1, Geological Society of America, 1957.

[15] J. Rodgers, "The distribution of marine carbonate sediments: A review," in *Regional Aspects of Carbonate Deposition*, R. J. L. Blanc and J. G. Breeding, Eds., 5: SEPM Society for Sedimentary Geology, 1957.

[16] R. C. T. Rainey, "Long-term changes in the earth's climate: Milankovitch cycles as an exercise in classical mechanics," *American Journal of Physics*, vol. 90, no. 11, pp. 848–856, 2022.

[17] Z. Liu, T. Hao, and G. Fan, "Geophysical study of sedimentary cycles," *Petroleum Geology & Experiment*, no. 3, pp. 258–262, 2004.

[18] S. Djin Nio, J. H. Brouwer, D. Smith, M. de Jong, and A. R. Böhm, "Spectral trend attribute analysis: Applications in the stratigraphic analysis of wireline logs," *First Break*, vol. 23, no. 4, pp. 71–75, 2005.

[19] S. Lu, H. Zhang, E. Meng, et al., "Application of INPEFA technique to carry out sequence-stratigraphic study," *Oil Geophysical Prospecting*, vol. 6, 2007.

[20] M. A. Bustillo, M. E. Arribas, and M. Bustillo, "Dolomitization and silicification in low-energy lacustrine carbonates (Paleogene, Madrid Basin, Spain)," *Sedimentary Geology*, vol. 151, nos. 1–2, pp. 107–126, 2002.

[21] C. Jia, C. Zou, J. Li, et al., "Assessment criteria, main types, basic features and resource prospects of the tight oil in China," *Acta Petrolei Sinica*, vol. 33, no. 3, pp. 343–350, 2012.

[22] P. Anadón, L. Cabrera, K. Kelts, et al., "International association of sedimentologists," in *Lacustrine facies analysis*, Blackwell Scientific, Oxford, 1991.

[23] M. J. Bojanowski, "Authigenic dolomites in the eocene–oligocene organic carbon-rich shales from the polish outer carpathians: Evidence of past gas production and possible gas hydrate formation in the Silesian Basin," *Marine and Petroleum Geology*, vol. 51, March, pp. 117–135, 2014.

[24] G. Song, X. Xu, Z. Li, et al., "Factors controlling oil production from paleogene shale in Jiyang depression," *Oil & Gas Geology*, vol. 36, no. 3, pp. 463–471, 2015.

[25] H. Liu, S. Hu, J. Li, et al., "Controlling factors of shale oil enrichment and exploration potential in lacustrine Bohai Bay Basin," *Natural Gas Geoscience*, vol. 30, no. 8, pp. 1190–1198, 2019.

[26] Y. Zhang, X. Qi, X. Cheng, et al., "Approach to sedimentary environment of late carboniferous-permian in Junggar Basin," *Xinjiang Petroleum Geology*, no. 6, pp. 673–675, 2007.

[27] Z. Yang, L. Hou, S. Lin, et al., "Geologic characteristics and exploration potential of tight oil and shale oil in Lucaogou formation in Jimsar Sag," *China Petroleum Exploration*, vol. 23, no. 4, pp. 76–85, 2018.

[28] L. Kuang, Y. Tang, D. Lei, et al., "Formation conditions and exploration potential of tight oil in the permian saline lacustrine dolomitic rock, Junggar Basin, NW China,"

Petroleum Exploration and Development, vol. 39, no. 6, pp. 700–711, 2012.

[29] X. Zhao, L. Zhou, X. Pu, et al., "Geological characteristics of shale rock system and shale oil exploration breakthrough in a lacustrine basin: A case study from the paleogene 1st submember of kong 2 member in Cangdong Sag, Bohai Bay Basin, China," *Petroleum Exploration and Development*, vol. 45, no. 3, pp. 377–388, 2018.

[30] C. Li, "Petroleum exploration history and enlightenment in Hailar Basin," *Xinjiang Petroleum Geology*, vol. 42, no. 3, 2021.

[31] C. Li, Q. Meng, D. Zhu, et al., "Prototype features and their controlling actions on the oil in Hailer-Tamutsag Basin," *Petroleum Geology*, vol. 33, no. 5, 2014.

[32] W. Wei, *The Origin of Complex Tight Reservoir of the Lower Cretaceous, Erlian Basin, China*, Docter, China University of Petroleum, Beijing, 2017.

[33] L. Song, C. Liu, H. Zhao, et al., "Geochemical characteristics, sedimentary environment and tectonic setting of Huangqikou Formation, Ordos Basin," *Earth Science*, vol. 41, no. 8, 2016.

[34] Y. Zhang, X. Hou, H. Zhang, et al., "Sedimentary characteristics and formation mechanism of peneprimary dolostone in the upper eocene salt-bearing interval in Qianjiang Sag, Jianghan Basin," *Journal of Palaeogeography*, no. 4, 2006.

[35] C. Lin, B. Wang, X. Zhang, et al., "Geological characteristics and paleoenvironmental significance of the paleogene lacustrine dolomite in the Beitang Sag, Bohai Bay Basin," *Geological Journal of China Universities*, vol. 25, no. 3, 2019.

[36] X. Liu, H. Jia, Y. Han, et al., "Origin of lacustrine dolostone in paleogene sha 4 member in Leijia area," *Global Geology*, vol. 38, no. 3, 2019.

[37] G. Wang, Q. Deng, and W. Tang, "The application of spectral analysis of logs in depositional cycle studies," *Petroleum Exploration and Development*, no. 1, pp. 93–95, 2002.

[38] J. Wang, *Sequence Stratigraphy of the Nantun Formation in Bayan Hushu Sag Division and Analysis of Reservoir Conditions*, Master, Changjing University, 2019.

[39] Y. Yuan, L. Wang, and R. Xie, "Application of INPEFA technology to sequence stratigraphy of the third member of funing formation, Nanhua block, Qintong Sag, north Jiangsu Basin," *Petroleum Geology & Experiment*, vol. 40, no. 6, 2018.

[40] F. A. Campbell and G. D. Williams, "Chemical Composition of Shales of Mannville Group (Lower Cretaceous) of Central Alberta, Canada." *AAPG Bulletin*, vol. 49, 1965.

[41] H. Deng and K. Qian, *Sedimentary Geochemistry and Environmental Analysis*, Gansu Science and Technology Press, Lanzhou, 1993.

[42] S. Wang, X. Huang, J. Tuo, et al., "Evolutional characteristics and their paleoclimate significance of trace elements in the hetaoyuan formation, Biyang depression," *Acta Sedimentologica Sinica*, no. 1, 1997.

[43] Y. Wang, W. Guo, and G. Zhang, "Application of some geochemical indicators in determining of sedimentary environment of funing group (paleogene), Jin-hu depression, Kiangsu province," *Journal of Tongji University*, no. 2, 1979.

[44] J. Yin, "An isotopic study of paleosalinity with Jurassic fossil shells," *Earh Science*, no. 5, 1988.

[45] H. Feng, J. Yu, Y. Fang, et al., "The palaeosaline analysis in the wufengian upper Yangtze Sea," *Journal of Stratigraphy*, no. 3, 1993.

[46] L. Peng, D. Han, R. Pu, et al., "W(sr)/W(ba) value of continental brackish lake deposit and its geological significance," *Journal of China University of Mining & Technology*, no. 1, 1999.

[47] R. Zheng and M. Liu, "Study on paleosalinity of change oil reservoir set in Ordos Basin," *Oil & Gas Geology*, no. 1, 1999.

[48] B. Jones and D. A. C. Manning, "Comparison of geochemical indices used for the interpretation of palaeoredox conditions in ancient mudstones," *Chemical Geology*, vol. 111, nos. 1–4, pp. 111–129, 1994.

[49] J. R. Hatch and J. S. Leventhal, "Relationship between inferred redox potential of the depositional environment and geochemistry of the upper Pennsylvanian (Missourian) stark shale member of the dennis limestone, Wabaunsee county, Kansas, U.S.A," *Chemical Geology*, vol. 99, nos. 1–3, pp. 65–82, 1992.

[50] X. Xiong and J. Xiao, "Geochemical indicators of sedimentary environment-a summary," *Earth and Environment*, vol. 39, no. 3, 2011.

[51] F. Chen, "Genesis and petroleum significant of calcareous mudstone strata of nantun Rouin Bei'er Sag," *Journal of Northeast Petroleum University*, vol. 39, no. 2, 2015.

[52] D. Zhong, Z. Jiang, Q. Guo, et al., "Discovery of hydrothermal dolostones in Baiyinchagan Sag of Erlian Basin, inner mongolia, and its geologic and mineral significance," *Oil & Gas Geology*, vol. 36, no. 4, 2015.

[53] Q. Guo, D. Zhong, F. Zhang, et al., "Origin of the lower cretaceous lacustrine dolostones in Baiyinchagan Sag of Erlian Basin, inner Mongolia," *Journal of Palaeogeography*, vol. 14, no. 1, 2012.

[54] G. Wang, R. Cheng, P. Wang, et al., "The forming mechanism of dolostone of Nengjiang formation in Songliao Basin - example from CCSD-SK ii," *Acta Geologica Sinica*, no. 1, 2008.

[55] Q. Meng, J. Li, Y. Li, et al., "Genetic mechanism of high content tuffaceous clastic rock reservoir in Hailar-Tamucage Basin," *Journal of Jilin University (Earth Science Edition)*, vol. 50, no. 2, pp. 569–578, 2020.